Analysis of Gene Expression Patterns and Chromosomal Changes Associated with Aging

Jochen B. Geigl,^{1,2} Sabine Langer,^{1,2} Simone Barwisch,^{1,2} Katrin Pfleghaar,^{1,2} Gaby Lederer,^{1,2} and Michael R. Speicher^{1,2}

¹Institute of Human Genetics, Technical University, Munich; and ²Institute of Human Genetics, GSF National Research Center for Environment and Health, Neuherberg, Germany

ABSTRACT

Age is the largest single risk factor for the development of cancer in mammals. Age-associated chromosomal changes, such as aneuploidy and telomere erosion, may be vitally involved in the initial steps of tumorigenesis. However, changes in gene expression specific for increased aneuploidy with age have not yet been characterized. Here, we address these questions by using a panel of fibroblast cell lines and lymphocyte cultures from young and old age groups. Oligonucleotide microarrays were used to characterize the expression of 14,500 genes. We measured telomere length and analyzed chromosome copy number changes and structural rearrangements by multicolor interphase fluorescence in situ hybridization and 7-fluorochrome multiplex fluorescence in situ hybridization, and we tried to show a relationship between gene expression patterns and chromosomal changes. These analyses revealed a number of genes involved in both the cell cycle and proliferation that are differently expressed in aged cells. More importantly, our data show an association between age-related aneuploidy and the gene expression level of genes involved in centromere and kinetochore function and in the microtubule and spindle assembly apparatus. To verify that some of these genes may also be involved in tumorigenesis, we compared the expression of these genes in chromosomally stable microsatellite instability and chromosomally unstable chromosomal instability colorectal tumor cell lines. Three genes (Notch2, H2AFY2, and CDC5L) showed similar expression differences between microsatellite instability and chromosomal instability cell lines as observed between the young and old cell cultures suggesting that they may play a role in tumorigenesis.

INTRODUCTION

The incidence of cancer rises with age (1). It is intriguing that aging is also associated with chromosomal changes, such as telomere attrition and increased aneuploidy, the presence of an extra or missing chromosome. Therefore, age-associated chromosomal changes may be critically involved in the initial steps of tumorigenesis.

In recent years, the association of telomere erosion and aging has been a focus of numerous studies, addressing both the importance of intact telomeres in maintaining chromosomal stability (2–4), as well as the possibility of dysfunctional telomeres resulting in aneuploidy and complex nonreciprocal translocations, which may therefore lead to cancer (4). In addition, aging has been linked to an increase in aneuploidy for the past several decades (5).

Because an euploidy has been suggested to be causative for cancer as it may induce genetic instability, such as chromosomal instability (6, 7), the present study set out to define the molecular mechanisms underlying age-associated an euploidy.

Recent reports identified genes of which the expression is associ-

Received 6/18/04; revised 8/31/04; accepted 10/5/04.

ated with age-related phenotypes and diseases (8, 9). In particular, it was suggested that an underlying mechanism of the aging process involves increasing errors of genes controlling the mitotic machinery of dividing cells (8). However, we show here that these previous studies are unsuitable to address the analysis of genes involved in the mitotic machinery, because existing differences between growth behavior of young and old cells were not considered. To achieve a more detailed, comprehensive analysis of age-related chromosomal changes and to monitor both structural and numerical chromosomal aberrations, we used gene expression profiling, telomere length measurements, and molecular cytogenetic assays. Experimental studies were done with six fibroblast cell cultures and eight lymphocyte preparations derived from young and old donors.

We identified 401 (2.8%) genes that were significantly differently regulated between young and old age groups. Correlating gene expression data with cytogenetic data enabled the identification of genes, which may be associated with age-related aneuploidy, many of which are involved in centromere and kinetochore function, as well as in the microtubule and spindle assembly apparatus. To begin to address the issue of whether these gene expression changes may also be involved in tumorigenesis, we compared the expression of these genes in 4 chromosomally stable microsatellite instability (RKO, DLD1, HCT116, and LOVO) and 3 chromosomally unstable chromosomal instability (SW480, HT29, and SW403) colorectal tumor cell lines. Three genes (Notch2, H2AFY2, and CDC5L) showed between microsatellite instability and chromosomal instability cell lines similar trends in different expression patterns as observed between the young and old cell cultures. Thus, these 3 genes may especially contribute to increased aneuploidy and, thus, eventual cancer with aging.

MATERIALS AND METHODS

Cell Samples. Five male primary human skin fibroblast cell lines (FY1-FY2 and FO1-FO3) were obtained from Coriell Cell Repositories (Camden, NJ). One male fibroblast cell line (FY3) was obtained from our institute's tissue repository (courtesy of Konstanze Hörtnagel). All of the fibroblast cell lines were classified into two groups: normal fibroblast young [FY: FY1 (Coriell cell repository number: GM083998/age: 8 years); FY2 (GM05757B/7 years); and FY3 (age given as "below 10 years")] and normal fibroblast old [FO: FO1(AG04064A/92 years); FO2 (AG12788A/90 years); and FO3 (AG07725B/91 years)].

Blood samples (30 mL) from apparently healthy female donors were obtained after informed consent and treated anonymously throughout the analysis. These samples were also classified into one group of normal lymphocyte young [LY: LY1 (29 years); LY2 (26 years); LY3 (25 years); and LY4 (26 years)] and into one group of normal lymphocytes old [LO: LO1 (96 years); LO2 (93 years); LO3 (91 years); and LO4 (92 years)].

In addition, we obtained 7 colorectal tumor cell lines. Four cell lines (RKO, DLD1, HCT116, and LOVO) are chromosomally stable and have microsatellite instability and 3 cell lines (SW480, HT29, and SW403) are known to have chromosomal instability (10).

Preparation of Fibroblasts and Blood Cells. Adherently growing fibroblasts were cultured in appropriate medium until confluency (\sim 60%), at which time the cells were harvested for chromosome preparation and DNA and RNA extraction.

Grant support: Deutsche Forschungsgemeinschaft (Sp 460/5–1) and the Bundesministerium für Bildung und Forschung (NGFN KB P06T5, P06T6).

The costs of publication of this article were defrayed in part by the payment of page charges. This article must therefore be hereby marked *advertisement* in accordance with 18 U.S.C. Section 1734 solely to indicate this fact.

Note: J. B. Geigl and S. Langer contributed equally to this work. Supplementary data for this article can be found at Cancer Research Online (http://cancerres.aacrjournals.org).

Requests for reprints: Michael R. Speicher, Institut für Humangenetik, Technische Universität München, Trogerstr. 32, D-81675 München, Germany. Phone: 49-89-4140-6381; Fax: 49-89-4140-6382; E-mail: speicher@humangenetik.med.tu-muenchen.de.

Mononucleated cells were obtained by Ficoll gradient separation and subsequently cultured for 72 hours with phytohemagglutinin stimulation. One flask of cells was used for chromosome preparation according to standard protocols, to estimate the mitotic index and the presence of structural aberrations and to determine telomere lengths. A second was used for DNA extraction to search for recurrent chromosomal imbalances by comparative genomic hybridization. The remaining flasks were used for RNA extraction and subsequent gene expression analysis.

Preparation of RNA and Microarray Hybridization. Sample preparation and processing was performed as described by the Affymetrix GeneChip Expression Analysis Protocols (Affymetrix Inc., Santa Clara, CA). Briefly, RNA was extracted with Trizol reagent 100 (Invitrogen, Karlsruhe, Germany) according to the manufacturer's instructions, repurified with phenol-chloroform extraction, and precipitated with propanol. The RNA pellet was then air-dried, resuspended in 15 to 30 μ L RNase-free H₂O, and its concentration determined by absorbance at 260 nm. RNA quality was verified by 28S and 18S rRNA integrity after ethidium bromide staining of total RNA samples denatured by formaldehyde agarose gel electrophoresis. Total cDNA was synthesized with a T7-polyT primer (Metabion, Martinsreid, Germany) with Superscript II choice for cDNA synthesis (Invitrogen) followed by *in vitro* transcription with biotinylated UTP and CTP (ENZO Life Sciences, Farmingdale, NY).

After hybridization to the human U133A GeneChip (Affymetrix), the chips were automatically washed and stained using Affymetrix fluidics station. Staining was performed using streptavidin phycoerythrin conjugate (SAPE, Molecular Probes, Leiden, The Netherlands) followed by the addition of biotinylated antibody (Vector Laboratories, Burlingame, CA) and finally treating with streptavidin phycoerythrin conjugate. The arrays were scanned using a Hewlett-Packard GeneArray Scanner 2500.

Microarray Data Analysis. Analysis was done using MicroArray Suite 5.0 (MAS, Affymetrix), dCHIP (11),³ and significance analysis of microarrays v1.13 (12).⁴

The default parameters of MAS were used for the statistical algorithm and for probe set scaling (with a target intensity of 500). The data were then filtered so that the absolute value of the fold change was >1.5 and the fold change probability value (p) was <0.05. Additionally, we removed genes that were scored as absent in experimental and baseline files (both numerator and denominator of the fold change), as well as those scored as increasing but absent in the experimental file (numerator of the fold change).

The .CEL files generated by MAS were converted into .DCP files using dCHIP, as described previously (11). The .DCP files were normalized, and raw gene expression data were generated using the dCHIP system of model-based analysis.

Comparisons of global gene expression profiles between young and old samples involved a two-pronged strategy. First, four young and four old lymphocyte samples were designated as "baseline" (B) and "experiment" (E), respectively. Genes that expressed 3-fold or higher in young *versus* old samples were then identified by defining the appropriate filtering criteria in the dCHIP software (mean E/mean B >3; mean E – mean B = 100, P < 0.1, t test). Second, young and old comparisons were also done using significance analysis of microarrays (12), which contain a sliding scale for false discovery rate of significantly up-regulated genes. We applied a false discovery rate threshold of 3.3% and a δ of 2.45. The results for both comparisons were similar; for simplicity we show here only the results obtained with significance analysis of microarrays.

Additional Microarray Information. The description of this microarray study followed the Minimum Information About a Microarray Experiment guidelines.⁵ We provide as supplemental material the raw data, normalization, and analysis of intra- *versus* inter-group variability with all of the genes identified in the study.

Preparation and Analysis of Metaphase Chromosomes, Multiplex-Fluorescence *In situ* Hybridization, and Comparative Genomic Hybridization. Preparation of metaphase spreads and GTG-banding analysis was done according to standard protocols. Twenty-four color karyotyping by multiplex-FISH (fluorescence *in situ* hybridization) was done with 7-fluorochromes as described (13). Metaphases were analyzed for the presence of chromosomal abnormalities, such as dicentric chromosomes and translocations using the Leica MCK-software (14). Comparative genomic hybridization was done according to standard protocols published previously. We used a Leica DM-RXA fluorescence microscope equipped with a Sensys charged coupled device (CCD) camera (Photometrics, Tucson, AZ).

Mitotic Index. The number of mitotic cells among 200 intact nuclei was obtained to produce the mitotic index.

Telomere Analysis by Quantitative-FISH on Metaphase Chromosomes. Quantitative-FISH analysis was performed as described previously (15). In brief, quantitative FISH was carried out on metaphase chromosomes using a FITC-labeled (CCCTAA)₃ PNA probe (DAKO, Glostrup, Denmark) according to the manufacturer's instructions. Digital images of metaphase spreads were recorded with an Axioplan II Imaging epifluorescence microscope equipped with a Axiocam-MRm CCD camera. Telomere profiles were analyzed with TFL-TELO V1.0a software (16). Quantitative-FISH analyses were performed on 10 to 15 metaphase spreads.

Apoptosis and Cell Proliferation Assay. The terminal deoxynucleotidyl-transferase-mediated dUTP nick end-labeling assay for DNA fragmentation was done using an *In situ* Death Detection kit (Roche), according to the manufacturer's instructions. Two hundred nuclei were evaluated with this assay. To assess proliferating cells, Ki67 staining was done according to the manufacturer's instruction (DAKO). We assessed 300 Ki67-stained nuclei.

Interphase Cytogenetics. In the male fibroblast cell lines, we used 10 different chromosome-specific centromere probes for our aneuploidy screen (chromosomes 3, 7, 8, 10, 11, 12, 17, 18, X, and Y). We prepared two five-color probe sets consisting of centromere probes for the following: (1) chromosomes 3, 10, 12, X, and Y, and (2) chromosomes 7, 8, 11, 17, and 18. Identical probes were used on female lymphocyte samples, except for the chromosome Y probe. Hybridization and signal quantitation was done as described (17).

RESULTS

The goal of our study was to compare gene expression changes associated with aging and their relationship to chromosomal pathologies. The starting material was composed of identical or similar human dermal fibroblast cell lines that had been proposed to represent an appropriate model system (8, 9).

Chromosomal Instability in Aging Fibroblast Cells. In normal cells, probes hybridizing to autosomes should yield two signals per cell, and probes hybridizing to sex chromosomes should, in male cells, yield one signal each per cell. Thus, the expected modal value for autosomal and sex chromosomes is two and one, respectively. The fraction of cells with signals above or below these modal values is a quantitative index of chromosomal instability (ref. 18; Fig. 1A and B). We observed a difference in the average chromosomal instability quantitative index between young and old fibroblast cells (2.2 and 4.4%, respectively; Table 1). Using the fraction of aneuploid and normal cells this difference was highly significant (Table 1).

Telomere Length and Structural Chromosomal Changes in Fibroblast Cells. To exclude the possibility of telomere erosion contributing to an increase in an euploidal cells from old donors, a quantitative image analysis was performed to estimate the telomere length. We found a highly significant difference in telomere length with increasing age, which was in agreement with previous reports (ref. 19; Fig. 1C). Average telomere lengths between young and old fibroblast cell lines were \sim 4,200 and 2,100 bps, respectively (P < 0.00001, Fisher's exact test).

Furthermore, dysfunctional telomeres may cause anaphase bridges, dicentric chromosomes, chromosomal fragmentation, and/or nonreciprocal translocations via a fusion-bridge breakage process (4). However, we found no indication for such changes using both standard cytogenetics banding methods and 7-fluorochrome multiplex-FISH, additionally validating that telomere erosion was not a contributing factor to aneuploidy in this fibroblast cell system.

³ Internet address: http://www.dCHIP.org.

Internet address: http://www-stat.stanford.edu/~tibs/SAM/.

⁵ Internet address: http://www.mged.org/Workgroups/MIAME/miame.html.

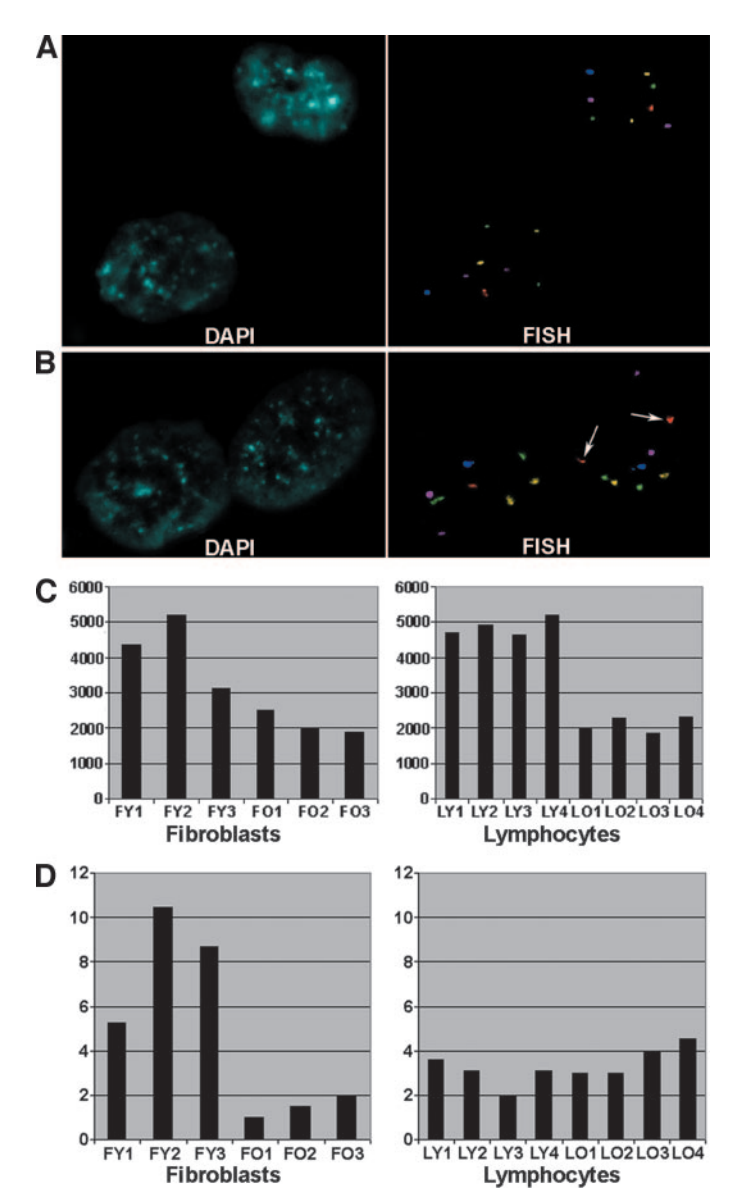


Fig. 1. A and B, representative interphase nuclei after hybridization with a centromere probe mix to nuclei of fibroblast cell line FY2 (A) and FO1 (B). The 4', 6-diamidino-2-phenylindole-stained nuclei are shown on the left; the right depicts corresponding signals for chromosomes 3 (green), 10 (pink), 12 (yellow), X (blue), and Y (red). All nuclei show two signals for chromosomes 3, 10, and 12. FY2 nuclei show as expected one signal each for the X and the Y chromosomes (A). In one nucleus of FO1 there are two signals for the Y chromosome (arrows) visible (B). C, estimation of telomere lengths using a PNA-TTAGGG probe. After quantitative FISH imaging the average telomere lengths were calculated in bp for the fibroblast cell cultures (left) and the lymphocyte cells (right). D, mitotic index observed in fibroblast cultures (left) and in lymphocyte cells (right).

Fibroblast Growth Behavior, Cell Morphology, and Mitotic Index. Similar or identical fibroblast cell lines have been used previously for gene expression profiling associated with aging (8, 9). However, a considerable problem occurs from the differing growth behavior between old and young cells. It has been noted previously that old fibroblasts possess a significantly higher proportion of cells exhibiting aberrant nuclear morphology, as compared with young fibroblasts (8), and additionally that the replicative potential of cells from normal old donors is reduced (9).

We confirmed this different growth behavior: The population doubling time for old fibroblasts was at least twice that of young fibroblasts. Furthermore, fibroblasts from old donors presented with a large proportion of cells (30–50%) displaying a postmitotic morphotype (20), which was associated with a senescent state. To additionally

confirm that old and young cells possess different replicative potentials, we determined the mitotic index. Indeed, we found considerable differences in the average mitotic index values between old and young fibroblasts (1.5 *versus* 8.2, respectively; P < 0.0001, Fisher's exact test; Fig. 1D).

Gene Expression Patterns in Fibroblasts. We reasoned that both the observed high percentage of senescent cells and different mitotic indices should be unsuitable for identifying gene expression changes involved in the mitotic machinery with aging, which was the main goal of our study. To confirm the results of Ly et al. (8), we restricted our examination to the transcriptional profiles of cell lines FY1 (GM083998) and FO3 (AG07725B), using the Affymetrix U133A-chip that is composed of 14,500 genes. Because gene expression data derived from two cell lines does not allow appropriate statistical analyses, we therefore compared the up- or down-regulation of genes proposed by Ly et al. (8) to be especially relevant for the mitotic machinery. As shown in Supplementary Table 1 we were indeed able to confirm their findings, which was particularly effective for those genes belonging to "cell cycle control proteins" and "chromosomal processing and assembly" groups.

An Alternative Cell System: Phytohemagglutinin-Stimulated Lymphocytes. Due to the above-mentioned significant differences in both growth rate and cell morphology of fibroblasts, we directed our attention to another cell system, based on the following considerations: (1) utilization of postadolescent young controls rather than children, to separate age-related from developmental changes (21), (2) selection of peripheral blood as cell source, as it is a uniquely accessible tissue, and (3) stimulation of lymphocytes by phytohemagglutinin, to obtain similar numbers of cycling cells irrespective of age. Because it should be generally difficult to effectively identify cell types in a natural context where both old and young cells show identical growth behavior, we reasoned that phytohemagglutinin stimulation should yield cell populations demonstrating similar cell cycle phases.

Lymphocyte Cell Cycle Phases. Establishment of cell cycle phases was accomplished by determining the mitotic index (Fig. 1D). Furthermore, the proliferative and apoptotic cell fractions were determined by Ki67 staining and terminal deoxynucleotidyltransferase-mediated dUTP nick end-labeling assay, respectively. Dissimilar Ki67-staining patterns corresponding to particular cell cycle phases (Fig. 2) enabled estimation of discrete cell cycle phases for each of the two young and two old lymphocyte cultures (Table 2). Cell percentages in respective phases were within similar range for all of the lymphocyte cultures. The only difference was for apoptotic cells, which were more frequently observed in lymphocytes from old as compared with young donors.

Chromosomal Instability in Lymphocytes. The average chromosomal instability quantitative index obtained from lymphocytes from young donors (2.6%; Table 1) was comparable with that from fibroblasts of young donors (2.2%). In contrast, we found an increase in the average chromosomal instability quantitative index in lymphocytes from old donors (20.1%; Table 1) and, furthermore, that the fraction of aneuploid cells was markedly higher in old lymphocytes than in old fibroblasts. This difference may likely reflect the equal proportion of cycling cells with lymphocytes in our experimental design. The difference between the fraction of aneuploid and normal cells was highly significant (Table 1).

It is noteworthy that no chromosome was immune from loss or gain. Chromosomes often reported to be typically lost in aging humans, such as one of the sex chromosomes, were not preferentially lost in our aneuploidy screening assay. To additionally verify the absence of preferential chromosomal gain or loss, we performed comparative genomic hybridization with DNA extracted from multi-

Table 1 Interphase nuclei were analyzed by interphase FISH using chromosome-specific centromere probes for chromosomes 3, 7, 8, 10, 11, 12, 17, 18, X, and Y

		Chromosomes										
		3	7	8	10	11	12	17	18	X	Y	Average
A. Cell culture	Mode	2	2	2	2	2	2	2	2	1	1	
Fraction												
FY1		5.1%	0.0%	1.1%	4.1%	2.2%	2.0%	3.2%	5.3%	3.1%	3.1%	2.92%
FY2		3.0%	5.1%	2.0%	2.0%	0.0%	1.0%	3.0%	1.0%	1.0%	3.1%	2.12%
FY3		3.1%	1.1%	2.2%	0.0%	2.2%	1.0%	2.2%	3.3%	0.0%	0.0%	1.51%
FO1		6.2%	5.0%	5.0%	12.5%	2.0%	4.1%	5.0%	1.0%	2.1%	9.3%	5.22%
FO2		7.3%	7.4%	3.2%	10.4%	2.2%	3.0%	2.1%	3.2%	1.0%	3.1%	4.29%
FO3		5.5%	2.3%	1.1%	6.6%	3.4%	5.5%	5.7%	4.6%	0.0%	2.2%	3.69%
	Mode	2	2	2	2	2	2	2	2	2		
Fraction												
LY1		3.0%	5.0%	0.0%	8.0%	4.0%	2.0%	3.0%	3.0%	3.0%		3.10%
LY2		ND	3.0%	1.0%	ND	4.0%	ND	1.0%	4.0%	ND		2.60%
LY3		1.0%	1.0%	1.0%	1.0%	0.0%	6.0%	1.0%	7.0%	3.0		2.10%
LY4		3.0%	2.0%	3.0%	4.0%	5.0%	1.0%	1.0%	4.0%	3.0		2.60%
LO1		ND	11.0%	14.0%	ND	33.0%	ND	5.0%	31.0%	ND		18.80%
LO2		14.0%	11.0%	14.0%	22.0%	33.0%	14.0%	5.0%	31.0%	37.0%		18.10%
LO3		27.0%	28.0%	21.0%	38.0%	12.0%	11.0%	14.0%	32.0%	29.0%		21.20%
LO4		30.0%	24.0%	16.0%	42.0%	12.0%	23.0%	25.0%	21.0%	29.0%		22.20%
B. Probe sets		Cell type		FY1-3	FO1-3		P value	LY1-4		LO1-4		P value
3, 10, 12, X, Y	7	F (aneuploid)		29	46		0.0356	45		232		< 0.0001
		F (normal)		255	237		355	168				
7, 8, 11, 17, 18	3	F (aneuploid)		27	62		< 0.0001	35		199		< 0.0001
		F (normal)		266	221		265	101				
Both probe		F (aneupl	oid)	56	1	108	< 0.0001	80		431		< 0.0001
Sets combined		F (norma	1)	521	458		620		269			

NOTE. In part A, for each chromosome tested, the modal number for fibroblasts and lymphocytes are shown as well as the fraction of cells of which the chromosome number is different from the mode. The 'average' value reflects the quantitative index of chromosomal instability used in this study. At least 100 nuclei were evaluated. In part B, to check whether the differences between young and old cell samples were statistically significant, we calculated the fraction of aneuploid [F(aneuploid)] and normal [F(normal)] cells for each of the two probes sets and for the combination of both probe sets. We applied the Fisher's exact test for two binominals. P < 0.05 were considered as significant. Abbreviations: ND, not done.

ple cells for each "old" donor. Such a gain/loss event of a given chromosome would result in a ratio shift of the respective chromosome. However, we found no such ratio shift event (data not shown).

Telomere Length and Structural Chromosomal Changes in Lymphocytes. Several studies have documented a progressive decrease in lymphocyte telomere length with advancing donor age (22). However, telomere length decrease in lymphocytes is a more complex event than in fibroblasts due to lymphocyte ability to up-regulate telomerase upon activation (23). Furthermore, the average telomere length in adult human lymphocytes is estimated to decrease by 1 kb every 20 to 50 years (23). This led to the speculation of whether chromosomal instability could be anticipated given this rate of telomere length loss over the course of a human life span.

Our study confirmed the progressive shortening of telomeres with aging (Fig. 1C), whereby the average length in old lymphocytes

compared with young was \sim 2,100 and 4,900 bp, respectively. Given these findings, it seems therefore unlikely that telomere erosion could have contributed to the observed aneuploidy. Consequently, neither standard chromosome banding analyses nor 7-fluorochrome multiplex-FISH could identify structural chromosomal changes, which have been discussed in the context of telomere abrogation (data not shown).

Lymphocyte Gene Expression. We characterized gene expression patterns associated with normal human aging by analyzing 14,500 transcribed genes. Before comparing gene expression patterns between lymphocytes from young and old donors, we constructed all of the possible donor pairs from the four members of each age group and compared the various pairs with each other using significance analysis of microarrays (12). Fig. 3A shows a typical comparison of two pairs of young to young donors. No significant gene expression changes

Fig. 2. Differential Ki67 staining patterns observed, which could be assigned to specific cell cycle stages as shown. Some cells had multiple, small Ki67 foci (first column) representing early G₁ phase. Cells in mid-G₁ phase were characterized by multiple small foci at the nuclear border and some intense Ki67 foci (second column). Cells in late G₁ and S phase demonstrated a few very intense Ki67 foci (third column). Early prophase cells or cells in the rosette phase showed homogenous Ki67 staining (fourth column). The vast majority of nuclei that were Ki67-negative (fifth column) correspond to G₀.

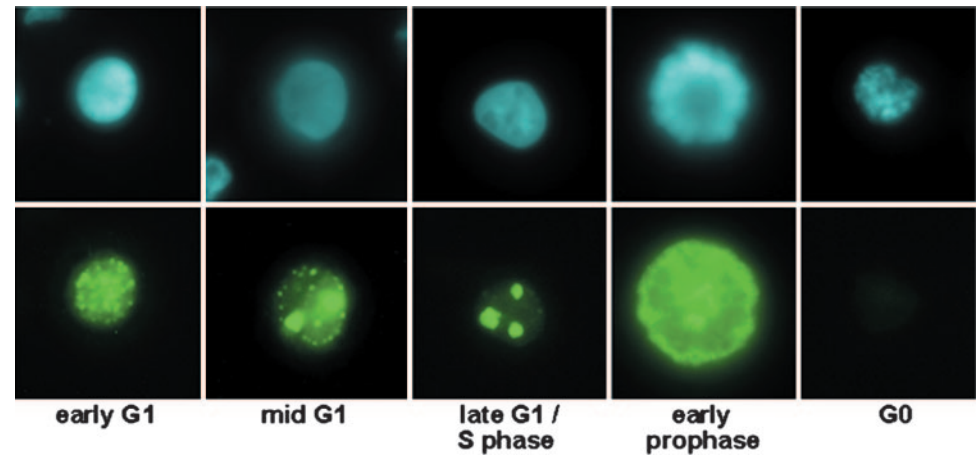


Table 2 Cell cycle phases of young and old lymphocytes (percentage)

Lymphocyte cell culture	G ₁ -G ₂ (Ki67 foci)	Early prophase (homogenous Ki67 staining)	Mitosis	G_0	Apoptosis
LY1	4.8	1.6	3.6	87.1	2.9
LY2	4.9	2.6	3.1	84.1	5.3
LO2	4.6	1.3	3.0	76.1	15.0
LO4	4.5	1.9	4.0	70.5	19.1

were detected. All of the other comparisons within young and old age groups yielded very similar results, so that there was no significant gene expression variability between individuals from the same age group.

In contrast, comparisons of gene expression patterns between old cells and baseline normal young cells resulted in 401 genes (2.8%) displaying at least a 1.5-fold difference, after application of a false discovery rate threshold of 3.3% and a δ of 2.4 (Fig. 3*B*).

Using the LocusLink database,⁶ we annotated function to 230 of 401 genes (57.4%) with possible known function. The functional categories of the differently expressed genes are summarized in Supplementary Table 2, and a full list of all 401 genes is shown in Supplementary Table 3.

Functional categorization of genes, which were differently regulated in cells from old donors, enabled us to speculate on pathways involved in aging and chromosomal pathology. Specifically, we were interested in genes that may explain age-associated aneuploidy. To this end, we identified a number of gene candidates involved in centromeres, kinetochores, microtubule and spindle assembly, and cell cycle and transcription, all of which may therefore affect chromosome segregation. The candidate genes most likely affecting aneuploidy, cell cycle regulation, and proliferation in aging cells are presented in Table 3.

Mitogen-Activated Protein Kinase Superfamily. We stimulated lymphocytes with phytohemagglutinin to obtain cycling lymphocytes. Phytohemagglutinin is a mitogen that preferentially stimulates T-lymphocyte mitosis, thus leading to a complex sequence of morphologic and biochemical events. phytohemagglutinin activates the mitogen-activated protein kinase superfamily (50), which itself is composed of three main protein kinase families: extracellular signal-regulated protein kinases, c-Jun NH₂-terminal kinases, and p38 family of kinases (51).

We wanted to exclude the possibility of differential stimulation of young and old lymphocytes by phytohemagglutinin and, thus, focused our analysis on gene expression patterns pertaining to genes of the mitogen-activated protein kinase-superfamily, as well as all of the other genes interacting with them (Supplementary Table 4). With the exception of DUSP4 (dual specificity phosphatase 4), no other genes were observed to differ consistently in expression between young or old cells, indicating that phytohemagglutinin stimulation did not have a significant effect with respect to age. DUSP4 may exert a negative regulation on mitogen-activated protein kinase superfamily members (51).

Potential Involvement of Gene Expression Differences in Tumorigenesis. To verify that some of these genes listed in Table 3 may also be involved in tumorigenesis, we compared the expression of these genes in chromosomally stable microsatellite instability and chromosomally unstable chromosomal instability colorectal tumor cell lines. For this, we used 7 colorectal tumor cell lines. Four cell lines (RKO, DLD1, HCT116, and LOVO) are chromosomally stable and have microsatellite instability (microsatellite instability) and 3 cell lines (SW480, HT29, and SW403) are known to have chromosomal instability (chromosomal instability; ref. 10). Gene expression

analysis was again done using the Affymetrix U133A chip. Three genes (*Notch2*, *H2AFY2*, and *CDC5L*) showed similar trends in gene expression differences between microsatellite instability and chromosomal instability cell lines as observed between the young and old cell cultures (data not shown).

DISCUSSION

The main goal of this study was to define genes that are associated with age-related aneuploidy. As such, this report compares global genome expression patterns across panels of normal fibroblasts and lymphocytes collected from donors of two different age groups. We also used highly sensitive molecular cytogenetic methodologies, including telomere length measurements and both multicolor interphase FISH and 7-fluorochrome multiplex-FISH to identify structural and numerical chromosomal aberrations. We observed a significant increase of aneuploid cells in aging. This chromosomal instability did not appear to be caused by telomere erosion.

The vast majority of epithelial tumors are characterized by a chromosomal instability of cancer cells, which is reflected as a plethora of numerical and structural chromosomal aberrations. Despite ongoing debate whether chromosomal changes reflect early or late events in tumorigenesis (52, 53), there is growing evidence that chromosomal alterations already exist in early forms of abnormal growth behavior, such as adenomas (54). It has been suggested that aneuploidy or chromosomal instability in tumor cells may be also caused by one dominant mutation (18). Candidate genes possibly leading to chromosomal instability in a monogenic and dominant fashion include *Bub1* (55), *Mad2* (56), *Securin* (57), and *hCDC4* (58). At the same time, the association between aging and an increased number of

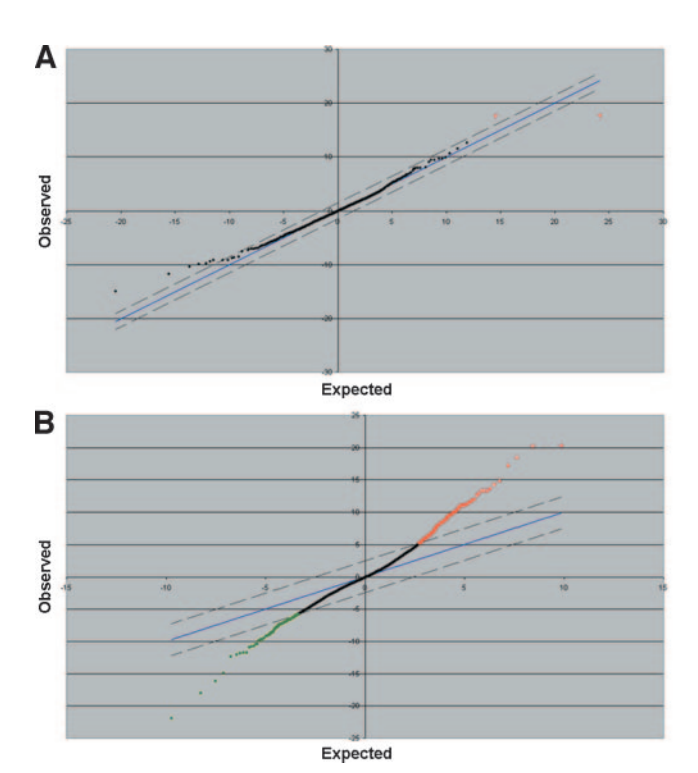


Fig. 3. Identification of genes with significant changes in expression. Shown are scatter plots of the observed relative difference (Y axis) versus the expected relative difference (X axis). The blue line indicates the point where the observed and expected relative differences are identical. The \(\delta\) values (distance between solid and dotted black lines) define the threshold for genes at which significant over- (shown in red) or underexpression (shown in green) was observed. For details see ref. 12. A, comparison of gene expression between 2 different young females. B, comparison of gene expression between 4 young and 4 old females.

⁶ Internet address: http://www.ncbi.nlm.nih.gov/LocusLINK//index.html.

Table 3 Gene expression in normal old cells relative to normal young cells: selection of genes that are differently expressed and that may specifically contribute to aneuploidy, cell cycle regulation, and proliferation

				Known function, disregulation may contribute to aneuploidy/	
Gene name	Synonym	GenBank	Fold change	cell cycle misregulation/aberrant cell proliferation	Reference
Centromere function					
Centromere protein C 1	CENPC1	M95724	+1.5	Formation of functional centromeres in eukaryotic organisms; maintaining proper kinetochore size and a timely transition to anaphase	(24)
DNA (cytosine-5-)-methyltransferase 3 β	DNMT3B	AF156487	-1.9	DNA methyltransferase; <i>de novo</i> methylation of major components of constitutive heterochromatin (satellites 2 and 3); centromeric instability	(25)
α Thalassemia/mental retardation syndrome X-linked	ATRX	U72937	+1.7	Associated with pericentromeric heterochromatin both in mitosis and during interphase; binding of kinetechore proteins	(26)
Spindle assembly and chromosome segregation ARP1 actin-related protein 1 homolog B	ACTR1B	X82207	+1.5	Encodes a subunit of dynactin; binds to microtubules; spindle formation and chromosome movement	(27)
Unc-84 homolog B	UNC84B	AB014568	+2.2	In <i>C. elegans</i> critical for microtubule binding and mitotic spindle assembly	(28)
Cyclin B1-gene	CCNB1	AI972071	-1.7	Essential component of the spindle-assembly checkpoint; important role in the G ₂ -M phase transition of the cell cycle	(29)
CDC5 cell division cycle 5-like gene Transcriptional activity/methylation	CDC5L	U86753	-1.6	G ₂ progression and entry into mitosis	(30)
H2A histone family, member Y2	H2AFY2	AF151534	+4.6	Establishing and/or maintaining transcriptionally silent chromatin domains	(31)
H3 histone, family 3A	H3F3A	D28384	+1.6	Packaging DNA into nucleosomal structures	(32)
Methyl CpG binding protein 2	MECP2	AF158180	+1.6	Belongs to a family of nuclear proteins related by the presence in each of a methyl-CpG binding domain; may serve as the bridge between histone modification enzymes and hypermethylated DNA; may be associated with gene inactivation	(33)
Cell growth, cell cycles, and cancer related genes					
Tousled-like kinase 1	TLK1	BC032657	+4.1	Coordinates cell cycle progression through the regulation of chromatin dynamics	(34)
Retinoic acid receptor responder (tazarotene induced) 3		AF060228	+2.8	Negative regulator of cell cycle and tumor suppression	(35)
Ras homolog gene family, member C	ARHC	BC009177	+2.5	Associated with progression of breast and ovarian cancer	(36)
p53 target zinc finger protein	WIG1	BC002896	+2.2	role in the p53-dependent growth regulatory pathway	(37)
Neuroblastoma, suppression of tumorigenicity 1	NBL1	AL703187	+1.9	Inhibitor or repressor in cell growth; negative regulation of cell cycle; possible tumor suppressing activity when overexpressed	(38)
Notch homolog 2 (Drosophila)	NOTCH2	U29680	+1.8	Can cause profound growth arrest, associated with G ₁ cell cycle block	(39)
RNA binding motif protein 5	RBM5	AF091263	+1.6	Overexpression suppresses cell proliferation by inducing apoptosis and by extending the G ₁ phase of the cell cycle	(40)
Heat shock protein 75	HSP75	AF154108	-1.7	May regulate Rb in response to progression of the cell cycle and to external stimuli	(41)
Hyaluronan-mediated motility receptor/RHAMM	HMMR	AF032862	-1.5	Acts transforming in fibroblasts	(42)
BCL2-related protein A1	BCL2A1	U29680	-1.9	Member of the BCL2 family of apoptosis regulators; has antiapoptotic activity	(43)
Period homolog 2	PER2	AB002345	-1.5	Functions in tumor suppression by regulating DNA damage- responsive pathways	(44)
Paired box gene 5	PAX5	U56835	-5.6	Transcription factor; may contribute to neoplastic transformation	(45)
High mobility group AT-hook 1	HMGA1	AK096863	-2.9	Regulation of inducible gene transcription, integration of retroviruses into chromosomes, and the metastatic progression of cancer cells	(46)
Related RAS viral (r-ras) oncogene homolog 2	RRAS2	BC013106	-1.9	Ras signaling pathway component	(47)
Nucleophosmin (nucleolar phosphoprotein B23, numatrin)		BC002398	-2.0	Crucial regulator of p53	(48)
Heat shock 70kDa protein 9B (mortalin-2)	HSPA9B	AU130219	-1.7	Inactivation of p53	(49)

NOTE. Fold difference in gene expression relative to normal young.

aneuploid cells has been known for decades. The rate of chromosomal gain and loss in normal aged cells is lesser than in chromosomal instability tumor cells, suggesting another mechanism as the possible cause of age-associated chromosomal instability.

At present we do not know whether a single gene may cause age-related aneuploidy. For example, a single gene could affect the regulation of all of the genes on our candidate list (Table 3). However, our data raise the possibility that age-related chromosomal instability may not be due to a single dominantly acting mutation but instead to combinatorial interactions between multiple genes. This includes misregulated genes affecting centromere function (e.g., CENPC1, DNMT3B, and ATRX) or spindle assembly and spindle assembly checkpoints (e.g., ACTRIB, UNC84B, and CCNB1). Moreover, a number of cancer-related genes were differently transcribed in aging cells (e.g., CCNB1, RARERES3, ARHC, NBL1, HSP75, and PAX5),

thus potentially further affecting cell cycle and cell proliferation (Table 3). It is intriguing that several genes that control epigenetic changes, such as methylation or histone modification (e.g., DNMT3B, H2AFY2, MECP2, and ATRX), also show a differential expression pattern between aging and young cells. Through their epigenetic effects, these genes may cause a different regulation of multiple genes in aging cells. This view is consistent with the observation that both increases and decreases in methylation occur with aging and may, in turn, have pathological consequences (59).

Of noteworthy mention was our capacity to identify another group of differentially regulated genes as that described previously (8). In this study, $\sim 1\%$ of the genes monitored showed reproducible expression level differences between various age samples, of which the majority were involved in mitosis and in extracellular matrix remodeling. However, due to the high percentage of senescent cells, a bias

contribution to the identification of differently expressed genes of the mitotic machinery with the fibroblast cell system cannot be excluded at this time.

Therefore, we redirected our attention to a different cell system and carried out phytohemagglutinin stimulation of lymphocytes to obtain cellular cycling irrespective of age. Our cell cycle analyses indicate that the various cycle phases were roughly equally represented across the two different age groups tested. Cells from old donors have a significantly higher rate of apoptosis, so some of the genes on the list (Table 3) could be related to this difference. We think that the increase of apoptotic cells is most likely a consequence of the higher percentage of aneuploid cells in cells from old donors. The aneuploidy will result in apoptosis in the majority of cells. Furthermore, we acknowledge herewith that an epithelial cell system may represent a more attractive experimental candidate, given our goal to draw conclusions regarding tumorigenesis usually being of epithelial origin. Notwithstanding, our observations with fibroblasts document the difficulties in performing appropriate studies using cells derived from solid organs. In contrast, phytohemagglutinin-stimulated lymphocytes demonstrated comparable growth patterns across cells derived from different age groups.

It is of interest that we observed a low variability of gene expression between individuals from the same age group despite earlier reports on differences in gene expression levels in mice (60) and in human lymphoblastoid cell lines (61).

To begin to address the issue of whether our list of candidate genes is meaningful and whether some of these genes may contribute to chromosomal instability in tumors, we additionally compared the gene expression pattern in 4 chromosomally stable microsatellite instability and 3 chromosomally unstable chromosomal instability colorectal cell lines. Three genes (*Notch2*, *H2AFY2*, and *CDC5L*) showed similar trends in gene expression differences between microsatellite instability and chromosomal instability cell lines as observed between the young and old cell cultures. This suggests that these genes may be a factor influencing chromosomal stability in tumorigenesis. An additional search of whether in chromosomally unstable tumors similar gene expression patterns are identified as in aging cells may provide further clues to the nature of chromosomal instability in human cancers.

ACKNOWLEDGMENTS

We are grateful to Claudia Wehner for help with expression analysis, Dr. Roland Lang and Jörg Mages for support with the array analyses, Dr. S. Wagenpfeil for aid with statistical analysis, and Dr. U. Olazabal for critical reading of the manuscript.

REFERENCES

- 1. DePinho RA. The age of cancer. Nature (Lond) 2000;408:248-54.
- Blasco MA, Lee HW, Hande MP, et al. Telomere shortening and tumor formation by mouse cells lacking telomerase RNA. Cell 1997;91:25–34.
- Rudolph KL, Chang S, Lee HW, et al. Longevity, stress response, and cancer in aging telomerase-deficient mice. Cell 1999;96:701–12.
- Artandi SE, Chang S, Lee SL, et al. Telomere dysfunction promotes non-reciprocal translocations and epithelial cancers in mice. Nature (Lond) 2000;406:641–5.
- Jacobs PA, Brunton M, Brown WMC, Doll R, Goldstein H. Change of human chromosome count distribution with age: evidence for a sex differences. Nature (Lond) 1963:197:1080.
- Duesberg P, Rausch C, Rasnick D, Hehlmann R. Genetic instability of cancer cells is proportional to their degree of aneuploidy. Proc Natl Acad Sci USA 1998;95: 13602-7
- Li R, Sonik A, Stindl R, Rasnick D, Duesberg P. Aneuploidy vs. gene mutation hypothesis of cancer: recent study claims mutation but is found to support aneuploidy. Proc Natl Acad Sci USA 2000;97:3236–41.
- Ly DH, Lockhart DJ, Lerner RA, Schultz PG. Mitotic misregulation and human aging. Science (Wash DC) 2000;287:2486–92.
- Kyng KJ, May A, Kolvraa S, Bohr VA. Gene expression profiling in Werner syndrome closely resembles that of normal aging. Proc Natl Acad Sci USA 2003; 100:12259-64.

- Abdel-Rahman WM, Katsura K, Rens W, et al. Spectral karyotyping suggests additional subsets of colorectal cancers characterized by pattern of chromosome rearrangement. Proc Natl Acad Sci USA 2001;98:2538–43.
- Li C, Wong WH. Model-based analysis of oligonucleotide arrays: Expression index computation and outlier detection. Proc Natl Acad Sci USA 2001;98:31–6.
- Tusher VG, Tibshirani R, Chu G. Significance analysis of microarrays applied to the ionizing radiation response. Proc Natl Acad Sci USA 2001;98:5116–21.
- Azofeifa J, Fauth C, Kraus J, et al. An optimized probe set for the detection of small interchromosomal aberrations by 24-color FISH. Am J Hum Genet 2000;66:1684–8.
- Eils R, Uhrig S, Saracoglu K, et al. An optimized, fully automated system for fast and accurate identification of chromosomal rearrangements by multiplex-FISH (M-FISH). Cytogenet Cell Genet 1998;82:160-71.
- Lansdorp PM, Verwoerd NP, van de Rijke FM, et al. Heterogeneity in telomere length of human chromosomes. Hum Mol Genet 1996;5:685–91.
- Poon SS, Martens UM, Ward RK, Lansdorp PM. Telomere length measurements using digital fluorescence microscopy. Cytometry 1999;36:267–78.
- Maierhofer C, Gangnus R, Diebold J, Speicher MR. Multicolor deconvolution microscopy of thick biological specimens. Am J Path 2003;162:373–9.
- Lengauer C, Kinzler KW, Vogelstein B. Genetic instability in colorectal cancers. Nature (Lond) 1997;386:623–7.
- Allsopp RC, Vaziri H, Patterson C, et al. Telomere length predicts replicative capacity of human fibroblasts. Proc Natl Acad Sci USA 1992;89:10114–8.
- Bayreuther K, Rodemann HP, Hommel R, Dittmann K, Albiez M, Francz PI. Human skin fibroblasts in vitro differentiate along a terminal cell lineage. Proc Natl Acad Sci USA 1988;85:5112–6.
- 21. Cristofalo VJ. A DNA chip off the aging block. Nat Med 2000;6:507.
- Weng NP, Levine BL, June CH, Hodes RJ. Human naive and memory T lymphocytes differ in telomeric length and replicative potential. Proc Natl Acad Sci USA 1995; 92:11091–4.
- Hodes RJ, Hathcock KS, Weng NP. Telomeres in T and B cells. Nat Rev Immun 2002;2:699–706.
- Trazzi S, Bernardoni R, Diolaiti D, et al. In vivo functional dissection of human inner kinetochore protein CENP-C. J Struct Biol 2002;140:39–48.
- Okano M, Bell DW, Haber DA, Li E. DNA methyltransferases Dnmt3a and Dnmt3b are essential for de novo methylation and mammalian development. Cell 1999;99: 247–57
- McDowell TL, Gibbons RJ, Sutherland H, et al. Localization of a putative transcriptional regulator (ATRX) at pericentromeric heterochromatin and the short arms of acrocentric chromosomes. Proc Natl Acad Sci USA 1999;96:13983–8.
- Clark SW, Staub O, Clark IB, et al. Beta-centractin: characterization and distribution
 of a new member of the centractin family of actin-related proteins. Mol Biol Cell
 1994;5:1301–10.
- Malone CJ, Fixsen WD, Horvitz HR, Han M. UNC-84 localizes to the nuclear envelope and is required for nuclear migration and anchoring during C. elegans development. Development 1999;126:3171–81.
- Chang DC, Xu N, Luo KQ. Degradation of cyclin B is required for the onset of anaphase in Mammalian cells. J Biol Chem 2003;278:37865–73.
- Bernstein HS, Coughlin SR. A mammalian homolog of fission yeast Cdc5 regulates G2 progression and mitotic entry. J Biol Chem 1998;273:4666–71.
- Costanzi C, Pehrson JR. MACROH2A2, a new member of the MARCOH2A core histone family. J Biol Chem 2001;276:21776–84.
- 32. Lin X, Wells DE. Localization of the human H3F3A histone gene to 1q41, outside of the normal histone gene clusters. Genomics 1997;46:526–8.
- Nan X, Ng HH, Johnson CA, et al. Transcriptional repression by the methyl-CpGbinding protein MeCP2 involves a histone deacetylase complex. Nature (Lond) 1998;393:386–389.
- Carrera P, Moshkin YM, Gronke S, et al. Tousled-like kinase functions with the chromatin assembly pathway regulating nuclear divisions. Genes Dev 2003;17: 2578-90
- DiSepio D, Ghosn C, Eckert RL, et al. Identification and characterization of a retinoid-induced class II tumor suppressor/growth regulatory gene. Proc Natl Acad Sci USA 1998:95:14811–5.
- Kleer CG, van Golen KL, Zhang Y, Wu ZF, Rubin MA, Merajver SD. Characterization of RhoC expression in benign and malignant breast disease: a potential new marker for small breast carcinomas with metastatic ability. Am J Pathol 2002;160: 579–84.
- 37. Hellborg F, Qian W, Mendez-Vidal C, et al. Human wig-1, a p53 target gene that encodes a growth inhibitory zinc finger protein. Oncogene 2001;20:5466-74.
- Enomoto H, Ozaki T, Takahashi E, et al. Identification of human DAN gene, mapping to the putative neuroblastoma tumor suppressor locus. Oncogene 1994;9:2785–91.
- Sriuranpong V, Borges MW, Ravi RK, et al. Notch signaling induces cell cycle arrest in small cell lung cancer cells. Cancer Res 2001;61:3200-5.
- Mourtada-Maarabouni M, Sutherland LC, Meredith JM, Williams GT. Simultaneous acceleration of the cell cycle and suppression of apoptosis by splice variant delta-6 of the candidate tumour suppressor LUCA-15/RBM5. Genes Cells 2003;8:109–19.
- Chen CF, Chen Y, Dai K, Chen PL, Riley DJ, Lee WH. A new member of the hsp90 family of molecular chaperones interacts with the retinoblastoma protein during mitosis and after heat shock. Mol Cell Biol 1996;16:4691–9.
- 42. Hall CL, Yang B, Yang X, et al. Overexpression of the hyaluronan receptor RHAMM is transforming and is also required for H-ras transformation. Cell 1995;82:19–26.
- D'Sa-Eipper C, Subramanian T, Chinnadurai G. bfl-1, a bcl-2 homologue, suppresses p53-induced apoptosis and exhibits potent cooperative transforming activity. Cancer Res 1996;56:3879–82.
- Fu L, Pelicano H, Liu J, Huang P, Lee C. The circadian gene Period2 plays an important role in tumor suppression and DNA damage response in vivo. Cell 2002; 111:41–50.

- Palmisano WA, Crume KP, Grimes MJ, et al. Aberrant promoter methylation of the transcription factor genes PAX5 alpha and beta in human cancers. Cancer Res 2003:63:4620-5.
- Sgarra R, Diana F, Bellarosa C, et al. During apoptosis of tumor cells HMGA1a protein undergoes methylation: identification of the modification site by mass spectrometry. Biochemistry 2003;42:3575–85.
- Kim R, Trubetskoy A, Suzuki T, Jenkins NA, Copeland NG, Lenz J. Genome-based identification of cancer genes by proviral tagging in mouse retrovirus-induced T-cell lymphomas. J Virol 2003;77:2056–62.
- 48. Colombo E, Marine JC, Danovi D, Falini B, Pelicci PG. Nucleophosmin regulates the stability and transcriptional activity of p53. Nat Cell Biol 2002;4:529–33.
- Wadhwa R, Yaguchi T, Hasan MK, Mitsui Y, Reddel RR, Kaul SC. Hsp70 family member, mot-2/mthsp70/GRP75, binds to the cytoplasmic sequestration domain of the p53 protein. Exp Cell Res 2002;274:246–53.
- Otte JM, Chen C, Brunke G, et al. Mechanisms of Lectin (Phytohemagglutinin)induced growth in small intestinal epithelial cells. Digestion 2001;64:169–78.
- Cowan KJ, Storey KB. Mitogen-activated protein kinases: new signaling pathways functioning in cellular responses to environmental stress. J Exp Biol 2003;206:1107–15.
- 52. Rajagopalan H, Nowak MA, Vogelstein B, Lengauer C. The significance of unstable chromosomes in colorectal cancer. Nat Rev Cancer 2003;3:695–701.

- Sieber OM, Heinimann K, Tomlinson IP. Genomic instability–the engine of tumorigenesis? Nat Rev Cancer 2003;3:701–8.
- Shih IM, Zhou W, Goodman SN, Lengauer C, Kinzler KW, Vogelstein B. Evidence that genetic instability occurs at an early stage of colorectal tumorigenesis. Cancer Res 2001;61:818–22.
- Cahill DP, Lengauer C, Yu J, et al. Mutations of mitotic checkpoint genes in human cancers. Nature (Lond) 1998;392:300–3.
- Michel LS, Liberal V, Chatterjee A, et al. MAD2 haplo-insufficiency causes premature anaphase and chromosome instability in mammalian cells. Nature (Lond) 2001; 409:355–9.
- Jallepalli PV, Waizenegger IC, Bunz F, et al. Securin is required for chromosomal stability in human cells. Cell 2001;105:445–57.
- Rajagopalan H, Jallepalli PV, Rago C, et al. Inactivation of hCDC4 can cause chromosomal instability. Nature (Lond) 2004;428:77–81.
- Richardson B. Impact of aging on DNA methylation. Ageing Res Rev 2003;2: 245–61.
- Pritchard CC, Hsu L, Delrow J, Nelson PS. Project normal: defining normal variance in mouse gene expression. Proc Natl Acad Sci USA 2001;98:13266–71.
- Cheung VG, Conlin LK, Weber TM, Arcaro M, Jen KY, Morley M, Spielman RS. Natural variation in human gene expression assessed in lymphoblastoid cells. Nat Genet 2003;33:422–5.